

U(1) spin liquids and valence bond solids in a large- N three-dimensional Heisenberg model

Jean-Sébastien Bernier,¹ Ying-Jer Kao,¹ and Yong Baek Kim^{1,2}

¹*Department of Physics, University of Toronto, Toronto, Ontario, Canada M5S 1A7*

²*School of Physics, Korea Institute for Advanced Study, Seoul 130-722, Korea*

(Dated: March 22, 2024)

We study possible quantum ground states of the $\text{Sp}(N)$ generalized Heisenberg model on a cubic lattice with nearest-neighbor *and* next-nearest-neighbor exchange interactions. The phase diagram is obtained in the large- N limit and fluctuation effects are considered via appropriate gauge theories. In particular, we find three U(1) spin liquid phases with different short-range magnetic correlations. These phases are characterized by deconfined gapped spinons, gapped monopoles, and gapless “photons”. As N becomes smaller, a confinement transition from these phases to valence bond solids (VBS) may occur. This transition is studied by using duality and analyzing the resulting theory of monopoles coupled to a non-compact dual gauge field; the condensation of the monopoles leads to VBS phases. We determine the resulting VBS phases emerging from two of the three spin liquid states. On the other hand, the spin liquid state near $J_1 = J_2$ appears to be more stable against monopole condensation and could be a promising candidate for a spin liquid state in real systems.

PACS numbers:

I. INTRODUCTION

The search for quantum spin liquid states in frustrated magnets has long been of great interest for condensed matter physicists. These exotic states exhibit fractionalized quantum numbers and may play important roles in understanding properties of novel complex materials such as high- T_c cuprates. In the spin liquid states, there exist deconfined spinons with spin quantum number $S = 1/2$, as opposed to the more familiar magnon excitations in the Néel state, or the spin triplet $S = 1$ excitations in the paramagnetic spin-Peierls states.¹ Previous studies of frustrated Heisenberg models on two dimensional lattices have revealed possible quantum spin liquid phases corresponding to the deconfined phases of Z_2 gauge theories.^{2,3,4,5} These phases are characterized by gapped spinons and gapped Z_2 -vortices that carry the Z_2 flux.^{6,7,8,9,10,11,12} Due to the gapped spectra of both spinons and Z_2 -vortices, it is difficult to observe an effect on measurable “local” quantities that distinguish the Z_2 spin liquid from a regular paramagnetic state. Theoretical proposals⁷ have been presented to observe the Z_2 -vortices; however, to this date, experimental attempts have shown negative results.¹³

U(1) analogues of these phases, the so-called U(1) spin liquids, are not stable due to instanton effects in two dimensions. On the other hand, deconfined phase of U(1) gauge theory can be stabilized in three dimensions (3D)^{14,15} and the resulting U(1) spin liquid states support gapped spinons, gapped monopoles, and gapless “photons”.^{16,17} Experimentally, these phases could be more easily observed since the gapless “photons” would show up in the low-energy physical properties of the system such as thermodynamics and energy/entropy transport. For example, an additional T^3 contribution to the specific heat from “photons” could be observed. There have been recent theoretical studies of three dimensional models in which possible U(1) spin liquid phases are identified.^{18,19,20} These models, however, are constructions in the limits where a large degeneracy in the ground state manifold is first achieved by hand; for example, in Ref 19, one needs to first take the easy-axis limit of the original Heisenberg model to facilitate

further analysis. One desires to obtain U(1) spin liquid phases without taking these special limits.

In this paper, we consider the $\text{Sp}(N)$ generalized three-dimensional frustrated Heisenberg model on a cubic lattice with nearest-neighbor (NN) J_1 and next-nearest-neighbor (NNN) J_2 interactions, using the bosonic $\text{Sp}(N)$ generalization of the physical spin $\text{SU}(2) = \text{Sp}(1)$ symmetry. Generalized spin operators can be expressed in terms of boson operators $b_i^\alpha; b_i^\beta$ at each site i where $\alpha = 1; \dots; 2N$ labels the $\text{Sp}(N)$ index, and the constraint $n_b = b_i^\alpha b_i^\alpha$ is imposed to fix the number of bosons per site ($n_b = 2S$ for $N = 1$ or the $\text{SU}(2)$ limit). This model has an advantage over other models as the spin-rotational symmetry is retained, and there is a direct connection with the microscopic model. We study the large- N limit of this model and examine the finite- N fluctuations via gauge theories. The phases obtained in the large- N limit could also be relevant to physical systems whose microscopic Hamiltonians are “near” the parameter space of the original Hamiltonian. This idea, for example, has been used to explain the observed spin-correlations in the 2D spin-liquid state in Cs_2CuCl_4 .^{21,22,23} Moreover, recent advances of trapped atoms in optical lattices²⁴ allow one to construct atomic systems with enhanced symmetries like $\text{Sp}(N)$ or $\text{SU}(N)$;²⁵ large- N theories would provide useful information about the ground states of such systems.

At the mean-field level, we solve the Hamiltonian in the $N \rightarrow 1$ limit with $n_b = N$ fixed. In general, smaller (larger) N corresponds to more (less) quantum fluctuations. As a result, magnetically long-range-ordered (LRO) phases appear in the large N limit and quantum-disordered paramagnetic phases arise in the small N limit. Moreover, different LRO and paramagnetic phases show up depending on the ratio J_2/J_1 . We find three different U(1) spin liquid states obtained by quantum-disordering LRO states with the ordering wave-vectors $(\pi; \pi; \pi); (0; \pi; \pi)$ and $(0; 0; \pi)$. These U(1) spin liquid phases are stable in the large- N limit due to gapped monopoles and still have short-range-ordered (SRO) spin correlations at the corresponding wave-vectors.

As N becomes smaller, however, monopoles may condense

by closing the gap, and confined phases such as valence bond solids (VBS) may arise. We examine possible monopole condensation patterns and find resulting VBS states that may emerge from the U(1) spin liquid phases. Different VBS phases are obtained from the U(1) spin liquid phases with the SRO correlations at (π, π) and $(0, 0)$. On the other hand, monopole condensation is not found in the U(1) spin liquid with $(0, \pi)$ SRO in the simplest consideration of monopole condensation. This may imply that one needs to go beyond the approximation schemes we used in the analysis, or this U(1) spin liquid phase near $J_1 = J_2$ is more stable against monopole condensation. If the latter is the case, this may be a more promising candidate for a U(1) spin liquid state in real materials.

The rest of the paper is organized as follows. In Sec. II, we introduce the formalism used in this work. In Sec. III, the large- N mean-field phase diagram is explained. In Sec. IV, fluctuation effects about the mean-field states are considered via U(1) gauge theory and its dual theory of monopoles coupled to a noncompact U(1) gauge field. Here, three U(1) spin liquid states are also identified. In Sec. V, possible VBS phases that may arise at finite- N are obtained using the dual theory of monopoles with frustrated hopping on the dual lattice. We conclude in Sec. VI.

II. FORMALISM

The Hamiltonian for our model can be written as

$$H = J_1 \sum_{\langle ij \rangle} S_i \cdot S_j + J_2 \sum_{\langle\langle ij \rangle\rangle} S_i \cdot S_j; \quad (1)$$

where S_i are $S = 1/2$ operators at site i . Here $J_1 > 0$ is the antiferromagnetic exchange coupling on the NN links, and $J_2 > 0$ on the NNN links. The proper description of a frustrated antiferromagnet requires that all spins transform under the same representation of a group, and two spins can combine to form a singlet. This requirement leads one to consider the generalization of the physical spin $SU(2) = Sp(1)$ symmetry to $Sp(N)$ and study the quantum ground states of the $Sp(N)$ Hamiltonian in the large- N limit.²

As the first step toward $Sp(N)$ generalization, one rewrites the $SU(2)$ spin operators using their bosonic representation, $S_i = \frac{1}{2} b_i^\dagger b_i$, where $b_i = \sum_{\alpha} b_i^\alpha$; $\alpha = \uparrow, \downarrow$ labels two possible spin states of each boson, b_i , and the constraint $n_b = b_i^\dagger b_i = 2S$ must be imposed at each site. The Heisenberg Hamiltonian, an additive constant aside, is then given by

$$H = \frac{1}{2} \sum_{\langle ij \rangle} J_{ij} (b_i^\dagger b_j^\dagger + b_i b_j) \quad (2)$$

where $J_{ij} = J_1$ is on the NN links, and $J_{ij} = J_2$ is on the NNN links. Here J_{ij} is the antisymmetric tensor of $SU(2)$. One can then generalize this expression to $Sp(N)$ by formally introducing N flavors of bosons on each site, and by changing

the constraint to $n_b = b_i^\dagger b_i = 2N S$, where $i = 1, \dots, 2N$ is the $Sp(N)$ index. For the physical case, $N = 1$, S takes half-integer values. Following these transformations, the $Sp(N)$ Hamiltonian becomes

$$H = \frac{1}{2N} \sum_{\langle ij \rangle} J_{ij} (b_i^\dagger b_j^\dagger + b_i b_j); \quad (3)$$

where $J_{ij} = J_{ji} = J$ is the generalization of the antisymmetric tensor of $SU(2)$; it is a $2N \times 2N$ matrix that contains N copies of J along its center block diagonal and vanishes elsewhere.²

In the $N \rightarrow 1$ limit at a fixed boson density per flavor, $n_b/N = 2S = 1$, we obtain to leading order in $1/N$ a mean field theory for $S = 1/2$. The fluctuations about the mean field solution give rise to a gauge theory.² The mean-field phase diagram at $N \rightarrow 1$ is shown in Fig. 1 as a function of $J_2 = (J_1 + J_2)$ and $1 = J_1/J_2$. At large values of S , various magnetically long-range-ordered (LRO) phases appear and are represented by the ordering wave-vector $q = (q_1, q_2, q_3)$. The short-range-ordered (SRO) phases at small values of S correspond to quantum-disordered phases with short-range equal-time spin correlations enhanced at the corresponding wave-vectors.

III. MEAN FIELD PHASE DIAGRAM

The mean-field theory can be obtained by decoupling the quartic boson interactions in S using Hubbard-Stratonovich fields $Q_{ij} = Q_{ji}$ directed along the lattice links. The effective action then contains the terms

$$S = \int d\tau \sum_{\langle ij \rangle} \frac{J_{ij}}{2} \text{Tr} [Q_{ij} (b_i^\dagger b_j^\dagger + b_i b_j) + \dots]; \quad (4)$$

where τ is the imaginary time and the ellipses represent standard terms which impose the canonical boson commutation relations and the constraint.² At the saddle point of the action, we get

$$Q_{ij} = \frac{1}{N} \sum_{\alpha} J_{ij} b_i^\alpha b_j^\alpha; \quad (5)$$

The one-site unit cell of the cubic lattice has nine of these Q_{ij} fields. For larger values of $S = 1/2$, the dynamics of S leads to the condensation of the b_i bosons and one obtains a nonzero value of

$$\langle b_i \rangle = x_i; \quad (6)$$

This corresponds to a magnetically-ordered phase.

The large- N limit of S is taken for a fixed value of $n_b/N = 2S$ and, depending on the ratio J_1/J_2 and the value of $1/N$, the ground state of S at $T = 0$ can either break the global $Sp(N)$ symmetry and possess magnetic LRO or be $Sp(N)$ invariant with only SRO. We optimized the ground state energy with respect to variations in Q_{ij} and x_i for different values of J_2/J_1 and $1/N$. We also found that each saddle point

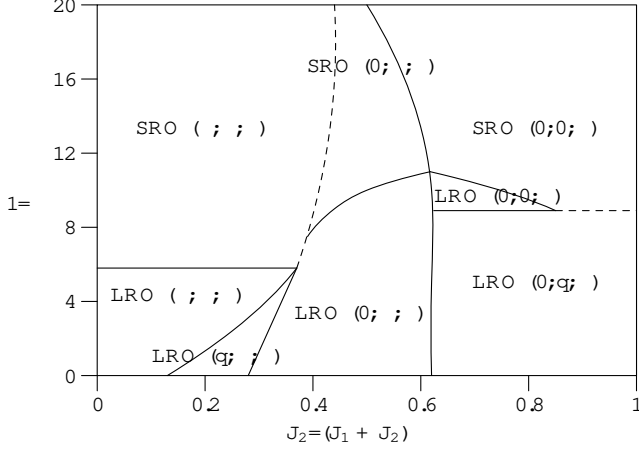


FIG. 1: Large- N phase diagram of the $Sp(N)$ cubic lattice model with first and second-nearest neighbor interactions as a function of $J_2 = (J_1 + J_2)$ and $1=$. The LRO phases break spin-rotation symmetry. The spin order is collinear and commensurate in the $(; ;)$, $(0; ;)$ and $(0;0;)$ LRO phases while it is helical and incommensurate in the $(q; ;)$ and $(0;q;)$ LRO phases. The SRO phases preserve spin-rotation invariance. Notice that the $(q; ;)$ and $(0;q;)$ LRO phases do not have SRO counterparts. [Dashed line: first order transition. Solid line: continuous transition.]

may be described by a purely real $\langle \mathbf{Q}_{ij} \rangle$. The phase diagram is summarized in Fig. 1. Notice the transition between different phases are in general second-order (solid lines), with the exception of two first-order transitions (dashed lines). The various magnetically ordered and paramagnetic phases are described in details as follows.

A. Magnetically ordered phases

The magnetically ordered phases are characterized by the finite condensate $\mathbf{x}_1 \neq 0$. In this model, we find the following LRO states.

1. $(; ;)$ LRO state

This is a long-range-ordered state in which $\langle \mathbf{S}_{ij} \rangle$ is collinearly polarized in opposite directions on two interpenetrating cubic sublattices (Fig. 2). A gauge can be chosen in which the expectation values of link variables are nonzero and equal on horizontal and vertical links, while the values on diagonal links are zero.

2. Helical $(q; ;)$ LRO state

This helically-ordered phase is characterized by nonzero values of $\langle \mathbf{Q}_{ij} \rangle$ on all NN links and on four faces of the cube (each face has two NNN links (Fig. 3)). In the appropriate gauge, two of the three possible NN bond directions present the same expectation value. Due to the three rotation axes of

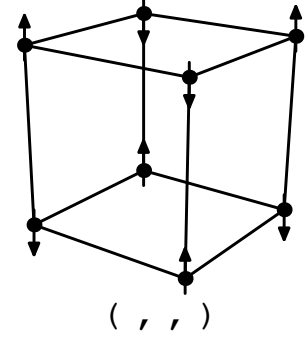


FIG. 2: $(; ;)$ phase. All NN bonds have nonzero values.

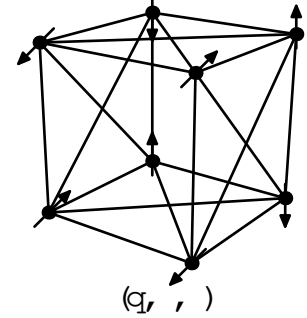


FIG. 3: $(q; ;)$ phase. All NN bonds have nonzero values and NNN bonds are nonzero on four of the six possible faces.

the cube, there are three possible choices for the nonequivalent NN link direction: $(q; ;)$; $(; q;)$; $(; ; q)$. This choice dictates on which four faces will lie the NNN bonds with nonzero expectation value. It is worth mentioning that all nonzero diagonal bonds have the same strength. Also, this phase has a long-range incommensurate spin order and the spin structure factor peaks at the incommensurate wave vector $(q; ;)$.

3. $(0; ;)$ LRO state

This magnetically ordered phase has nonzero bond expectation values for two of the three possible NN bond directions. Moreover, NNN links are nonzero and equal on four faces of the cube (Fig. 4). Once again, there are three possible choices of direction for the zero NN bond since these three configurations are interchangeable under rotation around the Cartesian axes of the cube.

4. $(0;0;)$ LRO state

This phase is characterized by nonzero NN bonds in only one of the three possible directions while NNN links are nonzero on four of the six faces (Fig. 5). There are three possible choices for the nonzero NN bond direction.

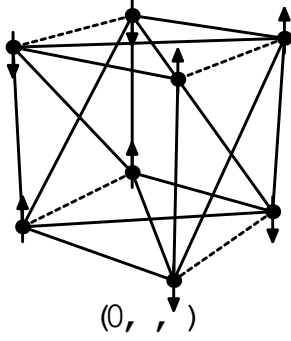


FIG. 4: $(0; q; r)$ phase. NN bonds are nonzero in two directions and NNN bonds are nonzero on four out of the six possible faces. [Note: dashed lines are only a guide to the eye.]

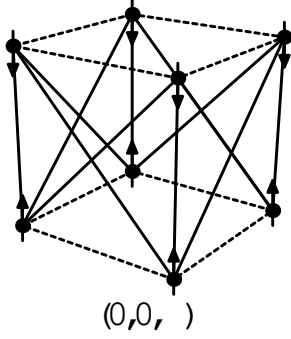


FIG. 5: $(0; 0; r)$ phase. Only NN bonds in one direction can be nonzero while NNN links are nonzero on four of the six faces. [Note: dashed lines are only a guide to the eye.]

5. Helical $(0; q; r)$ LRO state

This helically-ordered phase presents nonzero expectation values for all NNN bonds, and two of the NN bond directions are also nonzero (Fig. 6). Diagonal bonds do not exhibit the same strength, and the NN bond values continuously decrease and reach zero at $J_1 = 0$. Moreover, this phase exhibits a long-range incommensurate spin order and the spin structure factor peaks at the incommensurate wave vector $(0; q; r)$.

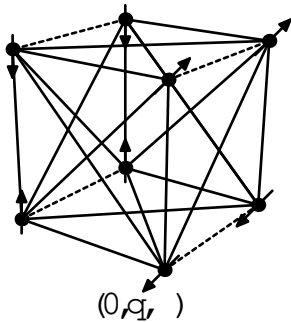


FIG. 6: $(0; q; r)$ phase. NN bonds are nonzero in two directions and decrease continuously as J_1 decreases. All NNN bonds are nonzero. [Note: dashed lines are only a guide to the eye.]

B. Paramagnetic phases

The paramagnetic phases are characterized by the vanishing condensate $\kappa_i = 0$ and a gapped spinon excitation spectrum. We find three distinct SRO states.

1. $(q; q; r)$ SRO state

This state is obtained by quantum disordering the $(q; q; r)$ LRO state. The expectation values of Q_{ij} have similar structures as those of its ordered counterpart. In this state, all spin excitations are gapped.

2. $(0; q; r)$ SRO state

Once again, this state is obtained by quantum disordering the corresponding LRO state. The expectation values of Q_{ij} have similar structures as those of its ordered counterpart. Although all spin excitations are gapped in this state, it is not symmetric under π -rotation around two of the Cartesian axes (y and z).

3. $(0; 0; r)$ SRO state

This state is the quantum disordered counterpart of the $(0; 0; r)$ LRO phase. The expectation values of the four NN links, not strictly null, are very small and will reach zero as J_1 decreases. Even though all spin excitations are gapped in this state, it is not symmetric under π -rotation around two of the Cartesian axes (x and y).

C. Analysis beyond mean-field for the paramagnetic phases

It is important to note that these three SRO phases possess bipartite lattice structure. To get a clearer picture, we label “up-spin” sites, where bosons carry a $+1$ “charge”, with A , and “down-spin” sites, where bosons carry a -1 “charge”, with B . Since all non-zero Q -fields are on bonds between A and B sublattices, these fields will form “charge”-zero objects. In other words, the mean field parameter $b_{Q_{ij}i}$ is invariant under a global $U(1)$ gauge transformation:

$$\begin{aligned} b_i &\rightarrow b_i e^{i\theta_i}; \\ b_j &\rightarrow b_j e^{-i\theta_j}; \\ Q_{ij} &\rightarrow Q_{ij}; \end{aligned} \quad (7)$$

where $i \in A$ and $j \in B$. Thus, unlike the Z_2 spin liquid cases in two-dimensions, the $U(1)$ symmetry of the action is intact. These phases would exhibit low-energy gapless $U(1)$ gauge excitations (“photons”).

However, to correctly capture the structure of these phases beyond the mean-field level, we also need to consider the contribution from topologically non-trivial gauge-field configura-

tions, namely monopoles. In particular, the interference effects between monopole events due to Berry phases lead to different quantum ground states. In general, two possible classes of paramagnetic ground states exist. In the first class of paramagnets, none of the symmetries of the Hamiltonian is broken. The spins are paired into valence bond singlets which strongly resonate between a large number of possible valence bond configurations. Such a state is a spin liquid or a resonating valence bond liquid. In the second class of paramagnets, the valence bond singlets spontaneously crystallize into a configuration which necessarily breaks a lattice symmetry. This configuration is a valence bond solid. We can distinguish these two classes of paramagnets using the expectation value of the monopole field as our order parameter. Monopoles are gapped in a spin liquid, and condense in a valence bond solid.

Consequently, in the next sections, we investigate under which conditions the three paramagnetic phases are spin liquids or valence bond solids. First, in section IV, we write down the action for such a system and find in which limit we get spin liquids. Then, in section V, we study the effect of monopole condensation and its consequence on the structure of the SRO phases.

IV. MONOPOLE ACTION, BERRY PHASES, AND U(1) SPIN LIQUIDS

The SRO phases described above have gapped spinons, hence we can safely integrate out spinons and study the resulting compact U(1) gauge theory.²⁶ This analysis was used successfully in (2+1)D to study antiferromagnets on the square²⁷, Shastry-Sutherland³, and checkerboard⁴ lattices. Thus, our starting point is the action of a compact U(1) gauge theory in (3+1)D on a space-time lattice in the presence of a Berry phase term. Physically, the Berry phase term can be assimilated to a static background gauge charge of strength 1 on the sites of the spatial cubic lattice. This action is given by

$$Z_A = \int_0^{2\pi} \prod_j d[A_j] \exp \left[K \sum_{\langle j,j' \rangle} \cos(A_j - A_{j'}) - i2S \sum_j A_j \right] \quad (8)$$

where j denotes the sites of the space-time lattice, and the cosine term represents the conventional Maxwell action for a compact U(1) gauge theory. It is the simplest local term consistent with the gauge symmetry $A_j \rightarrow A_j + 2\pi$ and it is periodic under $A_j \rightarrow A_j + 2\pi$. The last term is the crucial Berry phase leading to large cancellations between different paths. The static background gauge charges, f_j , can be 1 depending on the underlying magnetic structure.

In (2+1)D, the presence of an alternating static background charge lead, in confined paramagnetic phases, to broken translational symmetry. Here, our aim is to extend this analysis to (3+1)D paramagnets by performing duality transformations on S . Neglecting the Berry phase term, the remaining compact U(1) gauge theory becomes a theory of point-like monopoles coupled to the dual non-compact U(1) gauge field.

However, the presence of the background charge complicates the situation. The Berry phase term corresponds to a dual magnetic flux emanating from the center of each dual cube. This flux alternates in sign following a pattern particular to each SRO phase. Thus, we expect to get, after a series of dual transformations on S , a theory of monopoles with frustrated hopping coupled to a non-compact gauge field. In the remainder of this section, we first explicitly show how to obtain the aforementioned monopole action. Then we present the conditions under which these SRO phases are U(1) spin liquids.

A. Duality transformations: path towards “frustrated” monopole action

As a first step, we replace the cosine interaction by a Villain sum over periodic Gaussians such that

$$\exp \left[K \sum_{\langle j,j' \rangle} \cos(A_j - A_{j'}) \right] \approx \sum_{\bar{q}_j} \exp \left[\frac{K}{2} (A_j - A_{j'} - 2\pi \bar{q}_j)^2 \right]; \quad (9)$$

where \bar{q}_j denotes the sites of the dual lattice. We then rewrite this expression using Poisson resummation formula

$$\exp \left[K \sum_{\langle j,j' \rangle} \cos(A_j - A_{j'}) \right] \approx \sum_{\bar{q}_j} \int_{-\infty}^{\infty} d\bar{f}_j \exp \left[\frac{K}{2} (A_j - A_{j'} - 2\pi \bar{q}_j)^2 + i2\pi \bar{f}_j \bar{q}_j \right]; \quad (10)$$

where \bar{f}_j lives on the links of the direct lattice. Following the change of variable $\bar{q}_j = A_j - A_{j'} - 2\pi \bar{q}_j$, we perform Gaussian integrals over the intermediate fields \bar{q}_j and obtain

$$\exp \left[K \sum_{\langle j,j' \rangle} \cos(A_j - A_{j'}) \right] \approx \sum_{\bar{f}_j} \exp \left[\frac{\bar{f}_j^2}{2K} + i\bar{f}_j (A_j - A_{j'}) \right]; \quad (11)$$

Upon performing these transformation on (8), the resulting partition function is

$$Z_A = \int_0^{2\pi} \prod_j d[A_j] \sum_{\bar{f}_j} \exp \left[\sum_{\langle j,j' \rangle} \frac{\bar{f}_j^2}{2K} + i\bar{f}_j (A_j - A_{j'}) - i2S \sum_j A_j \right]; \quad (12)$$

where the integer-valued field \bar{f}_j can be interpreted as an analogue of the electromagnetic field tensor. For completeness, it should be noted that we dropped in Eq. (12) an insignificant overall normalization constant.

We can then perform on this more amenable expression the integrals over A_j , and we find (for $S = 1=2$) the condition

$$f_j = j : \quad (13)$$

This condition can take the form

$$\begin{aligned} e_{ja} &= j \\ \sum_{abc} b_{jc} e_{ja} &= 0 \end{aligned} \quad (14)$$

where e_{ja} is the “electric field” on the links of the direct lattice and b_{ja} is the “magnetic field” on the links of the dual lattice. Upon solving these two equations, we obtain

$$\begin{aligned} e_{ja} &= e_{ja}^0 + \sum_{abc} b_{jc} h_{ja} \\ b_{ja} &= h_{ja} + \sum_a j : \end{aligned} \quad (15)$$

Thus, $\sum_a e_{ja}^0 = j$, and we can rewrite the partition function in terms of e_{ja} and b_{ja}

$$\begin{aligned} Z_A &= \sum_{f_{ja}, b_{ja}, g} \exp \left[\frac{1}{2K} \sum_{j;a} (e_{ja}^2 + b_{ja}^2) \right] \\ &= \sum_{f_{ja}, h_{ja}, j;a, g} \exp \left[\frac{1}{2K} \sum_{j;a} (e_{ja}^0 + \sum_{abc} b_{jc} h_{ja})^2 \right] \\ &\quad + \left(\sum_a h_{ja} + \sum_a j \right)^2 : \end{aligned} \quad (16)$$

The physical properties of the partition function become clearer by parameterizing the “frustration” e_{ja}^0 into a curl in terms of a new fixed field Y_{jc} . Thus,

$$e_{ja}^0 = \sum_{abc} b_{jc} Y_{jc} : \quad (17)$$

Inserting Eq. (17) into Eq. (16), we can now write the partition function in the following form:

$$\begin{aligned} Z_A &= \sum_{f_{ja}, h_{ja}, j;a, g} \exp \left[\frac{1}{2K} \sum_{j;a} ((\sum_{abc} b_{jc} (h_{ja} + Y_{jc}))^2 \right. \\ &\quad \left. + (\sum_a h_{ja} + \sum_a j)^2) : \end{aligned} \quad (18)$$

To write Eq. (18) in a simpler form, we define a new dual field $L_{ja} = h_{ja} + Y_{ja}$, and make the gauge choice $j = L_{ja}$. As a result, our theory is now given by

$$Z_A = \sum_{f_{L_{ja}}, g} \exp \left[\frac{1}{2K} \sum_{j; <} (L_{ja} - L_{ja})^2 \right] : \quad (19)$$

We then promote the integer-valued field L_{ja} to real values with appropriate conditions. To do so, we first use the Poisson resummation formula to soften the integer constraint on L_{ja} . The cost of this procedure is the introduction of a new integer-valued field $J_j^{(m)}$, the monopole four-current. After shifting the real field by $L_{ja} \rightarrow L_{ja} + Y_{ja}$, we obtain

$$\begin{aligned} Z_A &= \sum_{f_{J_j^{(m)}}, g} \sum_{j; <} \exp \left[\frac{1}{2K} \sum_{j; <} (L_{ja} - L_{ja})^2 \right. \\ &\quad \left. + 2i \sum_{j; <} J_j^{(m)} (L_{ja} + Y_{ja}) \right] : \end{aligned} \quad (20)$$

Then, to control the fluctuations of $J_j^{(m)}$, we add the mass term

$$S_{\text{fugacity}} = \frac{\ln(m)}{2} \sum_{j; <} (J_j^{(m)})^2 : \quad (21)$$

Moreover, to explicitly make the the dual theory gauge invariant and to enforce monopole current conservation, we add a second term given by

$$\sum_{j; <} \exp \left[2i \sum_{j; <} J_j^{(m)} \right] : \quad (22)$$

where $J_j^{(m)}$ is a $U(1)$ field existing on each site of the dual lattice. Note that $\exp(i \sum_{j; <} J_j^{(m)})$ corresponds to the monopole creation operator and m is the monopole fugacity.

Following these two transformations, the partition function is now given by

$$Z_A = \sum_{f_{J_j^{(m)}}, g} \sum_{j; <} \exp \left[\frac{1}{2K} \sum_{j; <} (L_{ja} - L_{ja})^2 \right. \\ \left. + 2i \sum_{j; <} J_j^{(m)} (L_{ja} + Y_{ja}) \right] : \quad (23)$$

$$\begin{aligned} S &= \frac{1}{2K} \sum_{j; <} (L_{ja} - L_{ja})^2 \\ &\quad + 2i \sum_{j; <} J_j^{(m)} (L_{ja} + Y_{ja}) : \end{aligned} \quad (24)$$

Finally, upon summing over $J_j^{(m)}$, and rescaling all fields by 2, the final action reads

$$Z_A = \sum_{j; <} \exp \left[\frac{1}{8K} \sum_{j; <} (\mathbb{E}_{ja} - \mathbb{E}_{ja})^2 \right. \\ \left. + 2i \sum_{j; <} \mathbb{E}_{ja} \right] : \quad (25)$$

$$\begin{aligned} S &= \frac{1}{8K} \sum_{j; <} (\mathbb{E}_{ja} - \mathbb{E}_{ja})^2 \\ &\quad + 2i \sum_{j; <} \mathbb{E}_{ja} : \end{aligned} \quad (26)$$

It is important to note that, since the static gauge charge at the center of each dual cube is 1, the quantity $\sum_{abc} b_{jc}$, interpreted as fluxes through the faces of the dual cubes, is defined modulo 2.

To summarize our result, the duality transformations on S yield a theory of monopoles with frustrated hopping on the dual lattice, coupled to a dual non-compact gauge field \mathbb{E}_{ja} . The “frustration” is encoded in the field \mathbb{E}_{ja} and arises from the Berry phase term.

B. U(1) spin liquids

From the final expression of the dual action, we see that, for m close to zero, the monopole field is gapped, and the non-compact dual gauge field is free. Thus, the resulting phase has gapped spinons, has gapped monopoles, has gapless photons, and respects all the lattice symmetries. This phase is a U(1) spin liquid. Thus, for small fugacity, all three SRO phases can be spin liquids. It is interesting to note that the sole inclusion of the NNN interaction in the cubic lattice has allowed us to find three neighboring spin liquid phases in the parameter space.

V. VALENCE BOND SOLIDS

When m becomes of order one, monopole condensation gives rise to phases with broken symmetries. In this section, we study different valence bond configurations that may arise from the three SRO phases. In order to achieve this, we first ignore the fluctuations of the dual gauge field $\mathbb{E}_{\vec{j}}$. Once the structure of the resulting slow fluctuation description is known, we may restore the field $\mathbb{E}_{\vec{j}}$. Hence, we begin our study with the following action

$$S = \sum_{\vec{j}} \cos \left(\frac{e_{\vec{j}}^{(m)}}{\mathbb{E}_{\vec{j}}} \right) \quad (27)$$

We then rewrite the cosine term using exponentials, and promote to a continuous variable. The action now takes the form:

$$S = \frac{m}{2} \sum_{\vec{R}} \left(e^{i \frac{e_{\vec{R}}^{(m)}}{\mathbb{E}_{\vec{R}}}} + c.c. \right) + \sum_{\vec{R}} \left(e^{i \mathbb{E}_{\vec{R}} \cdot \vec{0}} e^{i \frac{e_{\vec{R}}^{(m)}}{\mathbb{E}_{\vec{R}}}} + c.c. \right); \quad (28)$$

where \vec{R} labels the sites on the cubic lattice dual to the original lattice of spins. The sites of the dual lattice are at the centers of the cubes defined by the planes of the original lattice, and $\vec{R} = (x; y; z)$ with x, y and z integers in units of the lattice constant ($a = 1$). Then, assuming that $e_{\vec{R}}^{(m)}$ is a slowly-varying function of time, we find

$$e^{i \frac{e_{\vec{R}}^{(m)}}{\mathbb{E}_{\vec{R}}}} + c.c. = 2 \mathbb{E}_{\vec{R}} e^{i \frac{e_{\vec{R}}^{(m)}}{\mathbb{E}_{\vec{R}}}} = 2 \mathbb{E}_{\vec{R}} \mathbb{J}_{\vec{R}}; \quad (29)$$

where $\mathbb{J}_{\vec{R}} = e^{i \frac{e_{\vec{R}}^{(m)}}{\mathbb{E}_{\vec{R}}}}$ is the monopole creation operator. Consequently, by dropping the constant term from Eq. (29) and adding the potential $V(\mathbb{J}_{\vec{R}}) = \tau_0 \mathbb{J}_{\vec{R}} + \tau_1 \mathbb{J}_{\vec{R}}^2 + \dots$; we obtain the continuous-time soft-spin action for the frustrated XY model

$$S = \sum_{\vec{R}} \mathbb{J}_{\vec{R}}^2 \sum_{\vec{R}} (\tau_{\vec{R}} \mathbb{J}_{\vec{R}} + \tau_1 \mathbb{J}_{\vec{R}}^2 + c.c.) + \sum_{\vec{R}} V(\mathbb{J}_{\vec{R}}); \quad (30)$$

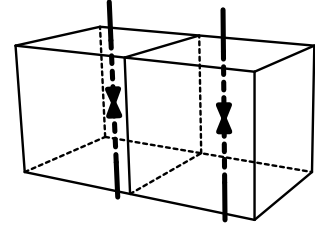


FIG. 7: Flux of $\mathbb{E}_{\vec{j}}$ through two of the six plaquettes of the dual lattice. There is no flux along the directions for which spins are not staggered.

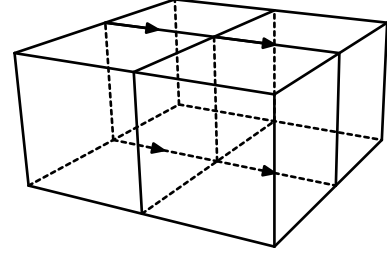


FIG. 8: A gauge choice for $\mathbb{E}_{\vec{j}}$ that realizes the fluxes shown in Fig. 7.

where the frustration is encoded in the monopole hopping amplitudes $t_{\vec{R}, \vec{R} + \vec{0}} = t e^{i \mathbb{E}_{\vec{R}} \cdot \vec{0}}$ corresponding to the fluxes through the dual plaquettes. These flux values depend on the fixed field $\mathbb{E}_{\vec{j}}$ which distinguishes the different SRO phases, and encapsulates the spin staggering in the local collinear order. It has the values

$$\mathbb{E}_{\vec{j}} = \begin{cases} (1) \hat{j}_z & \text{for } (0; 0;) \text{ SRO} \\ (1) \hat{j}_y + \hat{j}_z & \text{for } (0; ;) \text{ SRO} \\ (1) \hat{j}_x + \hat{j}_y + \hat{j}_z & \text{for } (; ;) \text{ SRO} \end{cases} \quad (31)$$

In the remainder of this section, we will find the possible monopole condensation patterns associated with the three SRO phases.

A. $(0; 0;)$ SRO

To analyze this SRO phase, we first need to find the monopole hopping amplitudes. To do so we choose an appropriate gauge (Fig. 8) that realizes the fluxes on the plaquettes, as shown in Fig. 7. The corresponding monopole hopping amplitude is given by

$$\begin{aligned} t_{\vec{R}, \vec{R} + \vec{x}} &= t e^{i \mathbb{E}_{\vec{R}} \cdot \vec{x}}; \\ t_{\vec{R}, \vec{R} + \vec{y}} &= t; \\ t_{\vec{R}, \vec{R} + \vec{z}} &= 1; \end{aligned} \quad (32)$$

where t and 1 are real-valued hopping coefficients. These coefficients emphasize the anisotropic character of the monopole hopping due to the presence of diagonal bonds on four faces of the cube. After diagonalizing the kinetic part of the soft-spin action Eq. (30), we find two low-energy modes. The normalized real-space wave functions associated with these two

monopole excitations carrying different lattice momenta are

$$\begin{aligned} \phi_1(\mathbf{R}) &= \frac{(1 + \frac{P}{2}) e^{i y}}{4 + 2 \frac{P}{2}} \\ \phi_2(\mathbf{R}) &= \frac{((1 + \frac{P}{2}) + e^{i y}) e^{i x}}{4 + 2 \frac{P}{2}} \end{aligned} \quad (33)$$

To characterize the behavior of this system near monopole condensation transition, we consider fields which are linear combinations of ϕ_1 and ϕ_2 . Any such linear combination is at the bottom of the monopole band where there is a continuum of states for the monopoles to condense:

$$\Phi(\mathbf{R}) = \phi_1 \phi_1(\mathbf{R}) + \phi_2 \phi_2(\mathbf{R}) \quad (34)$$

The phase transition in this system can be explored within a Ginzburg-Landau theory by treating ϕ_1 and ϕ_2 as slowly-varying fields. To simplify the next calculations, we define two new fields in terms of ϕ_1 and ϕ_2 :

$$\psi_1 = \phi_1 + i \phi_2; \quad \psi_2 = \phi_1 - i \phi_2; \quad (35)$$

By studying the action of the lattice symmetries, we find that the resulting Ginzburg-Landau functional is required to be invariant under the following transformations:

$$\begin{aligned} T_x : \quad & \begin{matrix} \psi_1 \rightarrow \psi_2 \\ \psi_2 \rightarrow \psi_1 \end{matrix} \\ T_y : \quad & \begin{matrix} \psi_1 \rightarrow i \psi_2 \\ \psi_2 \rightarrow -i \psi_1 \end{matrix} \\ T_z : \quad & \begin{matrix} \psi_1 \rightarrow \psi_1 \\ \psi_2 \rightarrow \psi_2 \end{matrix} \\ R_{=2; R_{xy}} : \quad & \begin{matrix} \psi_1 \rightarrow e^{i \frac{\pi}{4}} \psi_1 \\ \psi_2 \rightarrow e^{i \frac{\pi}{4}} \psi_2 \end{matrix} \\ R_{=2; R_{xz}} : \quad & \begin{matrix} \psi_1 \rightarrow \frac{1}{2} (\psi_1 + \psi_2 + (\psi_1 - \psi_2) (1)^{x+z}) \\ \psi_2 \rightarrow \frac{1}{2} (\psi_1 + \psi_2 - (\psi_1 - \psi_2) (1)^{x+z}) \end{matrix} \end{aligned} \quad (36)$$

where the $=2$ rotations are about the lattice points on which the monopoles reside. These transformations suggest that the simplest invariant takes the form

$$J(\psi_1; \psi_2) = N_x^2 N_y^2; \quad (37)$$

with

$$N = (\psi_1; \psi_2) \cdot \hat{y} \cdot \hat{z}; \quad (38)$$

where \hat{y} and \hat{z} are Pauli matrices. We then write down the continuum action for the two-component complex field $(\psi_1; \psi_2)$ that respects the above symmetries. In doing so, we have restored the dual gauge field \mathbf{L} and included some generic kinetic energy S_L for \mathbf{L} .

$$\begin{aligned} S_{\text{slow}} = \int d^3x \quad & \alpha^2 \mathbf{R} \cdot \mathbf{j}(\mathbf{r}) \cdot i \mathbf{L} + U(\mathbf{j} \cdot \mathbf{j}) + w J(\psi_1; \psi_2) \\ & + S_L; \end{aligned} \quad (39)$$

where $U(\mathbf{j} \cdot \mathbf{j}) = r \mathbf{j} \cdot \mathbf{j} + u \mathbf{j} \cdot \mathbf{j}^2 + \dots$. When $r < 0$, the monopoles would condense. From now on, we study confining paramagnetic phases originating from the Coulomb phase

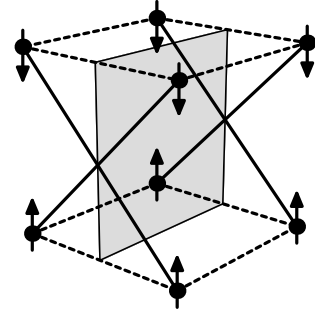


FIG. 9: Picture of a “sheet-like” columnar VBS state obtained when $w > 0$. The monopole density is increased on the x -odd planes which is interpreted as having antiferromagnetic bonds between NNN spins preferentially crossing these planes. [Note: dashed lines are only a guide for the eye.]

(U(1) spin liquid) by condensing single monopoles. Ground states are selected by minimizing $w J(\psi_1; \psi_2)$, and the sign of w determines the structure of the resulting phase.

The expectation values N_x and N_y are sufficient to characterize each state since the spatial monopole density is given by

$$\langle \mathbf{j}(\mathbf{R}) \cdot \mathbf{j} \rangle = C \frac{1}{2} \mathbf{j} \cdot \mathbf{j} \left((1 + \frac{P}{2}) ((1)^y N_x + (1)^x N_y) \right); \quad (40)$$

where C is a normalization constant. Depending on the sign of w , the following phases are possible.

$$I. \quad w > 0$$

In this case, there are four ground states

$$(N_x; N_y) = (1; 0); (0; 1); (0; 0); (1; 1); \quad (41)$$

For each state, the monopole density is the same in every other plane perpendicular to the x or y lattice axis. For example, the state $(N_x; N_y) = (0; 1)$ has an increased density on the x -odd planes and a decreased density on the x -even planes. In the original spin model, these dual planes are crossed by antiferromagnetic bonds between NNN spins, and there is an increased bond energy crossing the x -odd planes. Hence, this state corresponds to a “sheet-like” columnar valence bond solid with columns of zigzagging dimer chains running along the z direction. These columns are called “sheet-like” because they lie entirely on the yz plane (as illustrated in Fig. 9).

$$2. \quad w < 0$$

In this case, there are four ground states

$$(N_x; N_y) = (1; 1); (1; 0); (0; 1); (0; 0); \quad (42)$$

For these states, the monopole density oscillates in the x and y directions. For example, the state $(N_x; N_y) = (1; 1)$ has

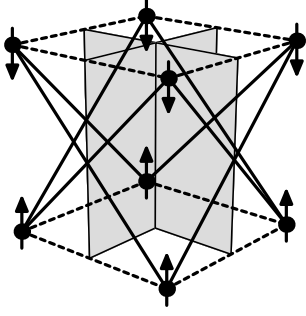


FIG. 10: Picture of “cylinder-like” columnar VBS state obtained when $w < 0$. The monopole density is increased on the x and y odd planes which is interpreted as having antiferromagnetic bonds between NNN spins preferentially crossing these planes. [Note: dashed lines are only a guide for the eye.]

increased density on odd x and y planes and decreased density on even x and y planes. In the original spin model, these dual planes are crossed by antiferromagnetic bonds between NNN spins, and there is an increased bond energy crossing the x and y odd planes. Consequently, this state corresponds to a “cylinder-like” columnar valence bond solid. As illustrated in Fig. 10, four connecting sheets of zigzagging dimer chains form a cylinder oriented along the z direction.

3. Connection to the VBS order parameter

Modulation of the monopole density in the dual lattice gives rise to the modulation of the dual gauge flux in the dual planes. The modulation of the dual gauge flux, in turn, corresponds to the modulation of static electric field on the links of the direct lattice. Following Ref. 28, we can identify the valence bond order parameter with these static electric fields. The valence bond order parameter in this phase, corresponding to diagonal bonds on the xz and yz faces of the cubic lattice, and links along the z direction, can be written as

$$\tilde{v}_{VBS} = \begin{pmatrix} 0 & 1 \\ (1)^x (S_r \ S_{r+\hat{x}+\hat{z}} + S_{r+\hat{z}} \ S_{r+\hat{x}}) & 1 \\ (1)^y (S_r \ S_{r+\hat{y}+\hat{z}} + S_{r+\hat{z}} \ S_{r+\hat{y}}) & A \\ (1)^z S_r \ S_{r+\hat{z}} & 0 \end{pmatrix} : \quad (43)$$

Using this observation, we can make the following identification, similar to that in Ref. 20,

$$\tilde{v}_{VBS} \sim \mathbf{N} = \mathbf{y} \sim : \quad (44)$$

Since the diagonal bonds occur in pairs, the perpendicular components of the spin correlations cancel, and we are left with the spin correlation along the link directions. Therefore the identification of the diagonal bond order parameter with the static electric fields in the link may be justified.

In the above analyses, there is no modulation of the monopole density in the z -direction; therefore, there is no valence bond solid order formation in the z -direction.

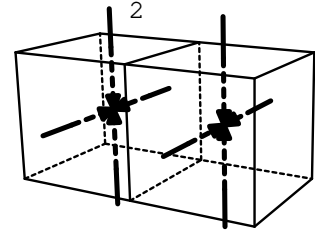


FIG. 11: Flux of $\frac{2}{z}$ through four of the six plaquettes of the dual lattice. There is no flux along the direction for which spins are not staggered.

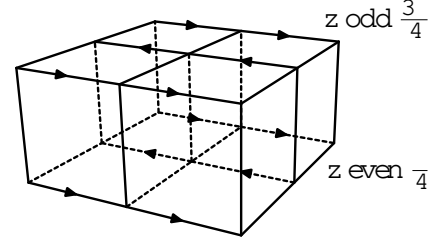


FIG. 12: A gauge choice for \mathbb{P}_j that leads to the fluxes shown in Fig. 11.

B. $(0; \frac{1}{2}; \frac{1}{2})$ SRO

In this phase, upon choosing an appropriate gauge (Fig. 12), the monopole hopping amplitudes (corresponding to the fluxes on the plaquettes as shown in Fig. 11) are given by

$$\begin{aligned} t_{R, R+\hat{x}} &= \frac{t}{2} e^{i z} + i e^{i y} ; \\ t_{R, R+\hat{y}} &= 1 ; \\ t_{R, R+\hat{z}} &= 1 ; \end{aligned} \quad (45)$$

where t and 1 are real-valued hopping coefficients. After diagonalizing the kinetic part of the soft-spin action Eq. (30), we find that the lowest energy band is dispersionless in the $(k_x; 0; 0)$ direction, as shown in Fig. 13. This indicates that there is a large degeneracy for the lowest lying mode at this level of approximation, and no monopole condensation can occur. By going beyond quadratic approximation, this mode may become dispersive again and we can then determine the correct monopole condensation pattern. Similar situations have been encountered in the studies of the quantum Ising model on a Kagome lattice,^{29,30,31} and numerical studies show that a valence bond solid with a larger unit cell is possibly the ground state. A similar structure might also be the ground state, at finite N , for our $(0; \frac{1}{2}; \frac{1}{2})$ SRO phase. This situation, however, could also be an indication that, at finite N , the spin liquid is more robust in the case of $(0; \frac{1}{2}; \frac{1}{2})$ SRO phase than it is for the other two SRO phases found in our study. Further studies are needed to properly determine the true ground state for this phase.

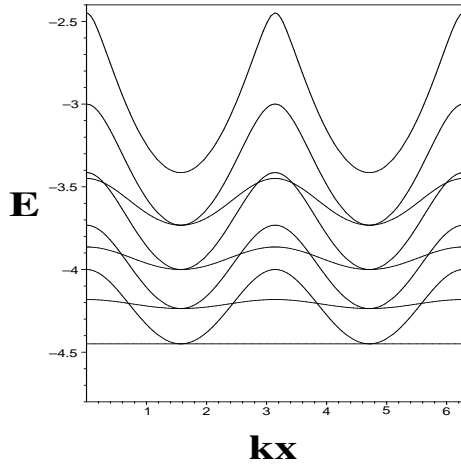


FIG. 13: Band structure given by the kinetic energy of the frustrated XY model in the $(0; \frac{1}{3}; 0)$ phase. Notice that the lowest energy band is flat in the $(k_x; 0; 0)$ direction. The second lowest band occurs for the k -vector $(k_x; \frac{1}{3}; 0)$.

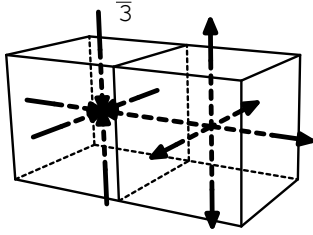


FIG. 14: Flux of $\frac{1}{3}$ through the six plaquettes of the dual lattice.

C. $(\frac{1}{3}; \frac{1}{3}; 0)$ SRO

Repeating the same procedure, we first find the monopole hopping amplitudes (corresponding to the fluxes on the plaquettes as shown in Fig. 14). Upon choosing the appropriate gauge (Fig. 15), these amplitudes are given by

$$\begin{aligned} t_{R;R+\hat{x}} &= \frac{r}{8} \frac{1}{3} \left(1 + ie^{i(x+y)} \right) + \frac{r}{8} \frac{1}{3} \left(1 - ie^{i(x+y)} \right) e^{iz}; \\ t_{R;R+\hat{y}} &= \frac{r}{8} \frac{1}{3} \left(1 - ie^{i(x+y)} \right) + \frac{r}{8} \frac{1}{3} \left(1 + ie^{i(x+y)} \right) e^{iz}; \\ t_{R;R+\hat{z}} &= 1; \end{aligned} \quad (46)$$

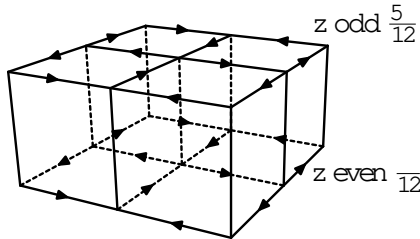


FIG. 15: A gauge choice for $\frac{1}{3}$ that realizes the fluxes shown in Fig. 14.

Similar monopole hopping problem was studied in the context of an interacting boson model.²⁰ As such, our analysis which follows shares some similarities with the discussions in the bosonic model,²⁰ and for completeness, we present relevant details of the analysis.

We diagonalize the kinetic energy and find two low-energy modes

$$\begin{aligned} \psi_1(R) &= \frac{1 + \left(\frac{1}{3} \frac{1}{2} \right) e^{iz}}{2 \left(\frac{1}{3} \frac{1}{6} \right)}; \\ \psi_2(R) &= \frac{1 - \left(\frac{1}{3} \frac{1}{2} \right) e^{iz}}{2 \left(\frac{1}{3} \frac{1}{6} \right)} \frac{e^{ix} \frac{1}{2} e^{iy}}{\frac{1}{2}}; \end{aligned} \quad (47)$$

Any linear combination of these two monopole excitations, as Eq. (48), is at the bottom of the monopole band. Hence, there is a continuum of states for the monopoles to condense.

$$\psi(R) = \psi_1(R) + \psi_2(R); \quad (48)$$

Near monopole condensation, we can analyze the transition using the Ginzburg-Landau formalism. By studying the action of the lattice symmetries, we notice that the resulting Ginzburg-Landau functional is required to be invariant under the following transformations:

$$\begin{aligned} T_x : & \begin{pmatrix} 1 & 1 \\ 1 & 1 \\ 1 & 2 \end{pmatrix} \rightarrow \begin{pmatrix} 2 & 2 \\ 2 & 2 \\ 2 & 1 \end{pmatrix} \\ T_y : & \begin{pmatrix} 1 & 1 \\ 1 & 1 \\ 2 & 1 \end{pmatrix} \rightarrow \begin{pmatrix} 2 & 2 \\ 2 & 2 \\ 1 & 2 \end{pmatrix} \\ T_z : & \begin{pmatrix} 1 & 1 \\ 2 & 1 \\ 1 & 2 \end{pmatrix} \rightarrow \begin{pmatrix} 1 & 2 \\ 1 & 2 \\ 2 & 2 \end{pmatrix} \\ R_{=2;R \times y} : & \begin{pmatrix} 1 & 1 \\ 1 & 1 \\ 1 & 2 \end{pmatrix} \rightarrow \begin{pmatrix} 1 & 1 \\ 2 & 1 \\ 2 & 2 \end{pmatrix} \\ R_{=2;R \times z} : & \begin{pmatrix} 1 & 1 \\ 2 & 1 \\ 1 & 2 \end{pmatrix} \rightarrow \begin{pmatrix} 1 & 2 \\ 1 & 2 \\ 2 & 2 \end{pmatrix} \end{aligned} \quad (49)$$

It appears from these transformations that the simplest invariant has the form

$$K(\psi) = N_x^2 N_y^2 + N_y^2 N_z^2 + N_z^2 N_x^2; \quad (50)$$

with

$$N(\psi) = \psi^\dagger \psi; \quad (51)$$

We then write down the continuum action for the two-component complex field $\psi(R)$ that respects the above symmetries. While doing so, we restore the dual gauge field L and include some generic kinetic energy for this field. The resulting action has the same form as the continuum action presented for the $(0; 0; 0)$ SRO phase (Eq. (39)), and, as before, the ground states are selected by minimizing $wK(\psi)$.

The expectation values N_x , N_y and N_z are sufficient to characterize each state since the spatial monopole density is given by

$$j(R)^2 = j^2 + \frac{1}{3} \left((1)^x N_x + (1)^y N_y + (1)^z N_z \right); \quad (52)$$

Then, according to the sign of w , we can find which valence bond solid structures are allowed.

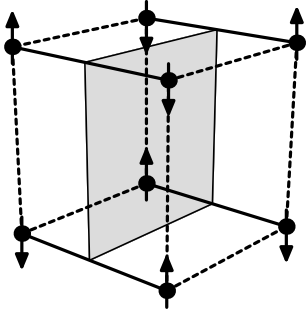


FIG. 16: Picture of a columnar VBS state obtained when $w > 0$. The monopole density is increased on the x -even planes which is interpreted as having antiferromagnetic bonds between NN spins preferentially crossing these planes. [Note: dashed lines are only a guide for the eye.]

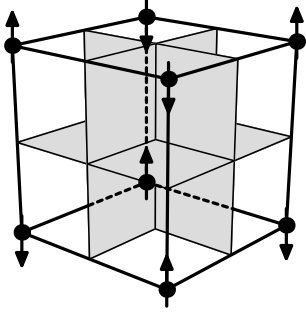


FIG. 17: Picture of a 3D box VBS state obtained when $w < 0$. The monopole density is increased on all x , y and z even planes, and the dimers resonate around cubes center where these three planes meet. [Note: dashed lines are parts of the real bonds.]

1. $w > 0$

In this case, there are six ground states

$$(\mathbb{N}_x; \mathbb{N}_y; \mathbb{N}_z) = (1; 0; 0); (0; 1; 0); (0; 0; 1); (53)$$

In a given state, the monopole density is the same in every other plane perpendicular to a fixed lattice axis. For example the state $(\mathbb{N}_x; \mathbb{N}_y; \mathbb{N}_z) = (1; 0; 0)$ has an increased density on the x -even planes and decreased density on the x -odd planes, as shown in Fig. 16. In the original spin model, these dual planes are crossed by antiferromagnetic bonds between NN spins, and there is an increased bond energy crossing the x -even planes. Hence, this state corresponds to a columnar valence bond solid with dimers oriented in the x direction.

2. $w < 0$

For this second case, there are eight ground states

$$(\mathbb{N}_x; \mathbb{N}_y; \mathbb{N}_z) = \frac{1}{\mathbb{P}=\frac{1}{3}} (1; 1; 1) \quad (54)$$

where each of the three signs can be chosen independently. The monopole density for these states is periodic in all three

directions and correspond to three-dimensional “box” valence bond solids. For example, the state $(\mathbb{N}_x; \mathbb{N}_y; \mathbb{N}_z) = \frac{1}{\mathbb{P}=\frac{1}{3}} (1; 1; 1)$ has maximal monopole density for even x , y and z , as shown in Fig. 17. In the original spin model, this state has dimers resonating around direct lattice cubes surrounding the dual lattice points.

VI. CONCLUSION

In this paper, we studied the quantum ground states of the $\text{Sp}(N)$ antiferromagnetic Heisenberg model on the cubic lattice with NN (J_1), and NNN (J_2) exchange interactions. This is the simplest 3D model with frustration. We have shown that the sole addition of the NNN interaction on the cubic lattice gave rise to three neighboring U(1) spin liquids with magnetic short-range correlations at $(\frac{1}{2}; \frac{1}{2}; \frac{1}{2}); (0; \frac{1}{2}; \frac{1}{2}); (0; 0; \frac{1}{2})$. Moreover, there are indications that $(0; \frac{1}{2}; \frac{1}{2})$ U(1) spin liquid is more likely to “survive” at finite N values. This model has an advantage over other models because of its direct connection to realistic microscopic models. Thus, verifying the results of our model in real systems would be more amenable.

We first obtained the mean-field phase diagram of this model in the $N \rightarrow 1$ limit as a function of $J_2 = (J_1 + J_2)$, which controls the frustration, and $1 = \frac{1}{N}$, which controls quantum fluctuations. For large values of $\frac{1}{N}$, we find various magnetically ordered phases; $(\frac{1}{2}; \frac{1}{2}; \frac{1}{2})$, $(0; \frac{1}{2}; \frac{1}{2})$, $(0; 0; \frac{1}{2})$ collinear-ordered and $(\frac{1}{2}; \frac{1}{2}; \frac{1}{2})$, $(0; \frac{1}{2}; \frac{1}{2})$ helically-ordered states. Upon decreasing $\frac{1}{N}$, we find three quantum-disordered paramagnetic phases (SRO) with enhanced spin correlations at $(\frac{1}{2}; \frac{1}{2}; \frac{1}{2}); (0; \frac{1}{2}; \frac{1}{2}); (0; 0; \frac{1}{2})$. Since these are quantum-disordered states of collinear-ordered magnets, we see already at the mean-field level that these phases are possible U(1) spin liquids.

Methods have been developed by Haldane,³² Read, and Sachdev²⁸ to study (2+1)D quantum antiferromagnets. In this work, we have extended these methods to (3+1)D and analyzed the effects of singular fluctuations about the mean-field states. These monopole events, or the topological defects in the U(1) gauge theory, represent tunneling between different topologically distinct sectors. We find that, when $N \rightarrow 1$ (small monopole fugacity), the three paramagnetic phases are indeed U(1) spin liquids. At finite N values (large monopole fugacity), the system may become confined due to monopole condensation, and we discover various possible VBS ordered phases for SRO $(\frac{1}{2}; \frac{1}{2}; \frac{1}{2})$ and $(0; 0; \frac{1}{2})$ states. However, it appears that, when $J_1 \approx J_2$, the corresponding U(1) spin liquid with $(0; \frac{1}{2}; \frac{1}{2})$ SRO seems to be more stable in the simplest consideration of monopole condensation than the two other spin liquid states. We would need a more elaborate analysis to determine the ultimate fate of this state. One possibility would be that it becomes a VBS state with a very large unit cell.^{29,30} Another possibility is that it remains a U(1) spin liquid near $J_1 \approx J_2$ even at finite N . If the latter is the case, this U(1) spin liquid may be a better candidate to be observed in real systems. One may be able to gain more insights on this issue using numerical methods.

It is worthwhile to mention that the U(1) spin liquids

studied previously, in the context of other three-dimensional models, correspond to our U(1) spin liquid with SRO (; ;).^{18,19,20,33} On the other hand, we find two other possible U(1) spin liquids with (0; ;) and (0;0;) correlations within our model. It is also interesting to note that our analysis for the quantum-disordered paramagnetic phases at finite N shares some similarities with the studies of an interacting boson system at half-filling.²⁰ The nature of the phase transitions between different U(1) spin liquid states and VBS phases is still not clear and awaits further investigation.

Acknowledgments

This work was supported by NSERC of Canada, Canada Research Chair program, Canadian Institute for Advanced Re-

search (YBK) and FQRNT-Québec (JSB). We would also like to thank O. Motrunich, T. Senthil, and M.P.A. Fisher for helpful discussions, and S. Takei for his technical assistance. YBK is grateful to Kavli Institute for Theoretical Physics and Aspen Center for Physics for their hospitality where some parts of this work were performed.

-
- ¹ S. Sachdev, *Quantum Phase Transitions* (Cambridge University Press, 1999).
 - ² S. Sachdev, Phys. Rev. B **45**, 12 377 (1992); N. Read and S. Sachdev, Phys. Rev. Lett. **66**, 1773 (1991); S. Sachdev and N. Read, Int. J. Mod. Phys. B **5**, 219 (1991); S. Sachdev, Annales Henri-Poincaré **4**, 559 (2003).
 - ³ C. H. Chung, J. B. Marston, and S. Sachdev, Phys. Rev. B **64**, 134407 (2001).
 - ⁴ J.-S. Bernier, C.-H. Chung, Y. B. Kim, and S. Sachdev, Phys. Rev. B **69**, 214427 (2004).
 - ⁵ L. Balents, M. P. A. Fisher, and S. Girvin, Phys. Rev. B **65**, 224412 (2002).
 - ⁶ T. Senthil and M. P. A. Fisher, Phys. Rev. B **62**, 7850 (2000).
 - ⁷ T. Senthil and M. P. A. Fisher, Phys. Rev. Lett. **86**, 292 (2001).
 - ⁸ D. S. Rokhsar and S. A. Kivelson, Phys. Rev. Lett. **61**, 2376 (1988).
 - ⁹ X. G. Wen, Phys. Rev. B **44**, 2664 (1991).
 - ¹⁰ R. Moessner, S. Sondhi, and E. Fradkin, Phys. Rev. B **65**, 024504 (2002).
 - ¹¹ C. Nayak and K. Shtengel, Phys. Rev. B **64**, 064422 (2001).
 - ¹² E. Demler, C. Nayak, H.-Y. Kee, Y. B. Kim, and T. Senthil, Phys. Rev. B **65**, 155103 (2002).
 - ¹³ D. A. Bonn, W. J. C. B. W. Gardner, Y.-J. Lin, R. Liang, W. N. Hardy, J. R. Kirtley, and K. A. Moler, Nature **414**, 887 (2001).
 - ¹⁴ A. M. Polyakov, *Gauge Fields and Strings* (Harwood Academic, New York, 1987).
 - ¹⁵ When the matter field has a gapless spectrum, it is possible to stabilize U(1) spin liquid in 2D. See M. Hermele *et al.*, cond-mat/0404751.
 - ¹⁶ X.-G. Wen, Phys. Rev. Lett. **88**, 011602 (2002).
 - ¹⁷ X.-G. Wen, Phys. Rev. B **68**, 115413 (2003).
 - ¹⁸ D. A. Huse, W. Krauth, R. Moessner, and S. L. Sondhi, Phys. Rev. Lett. **91**, 167004 (2004).
 - ¹⁹ M. Hermele, M. P. A. Fisher, and L. Balents, Phys. Rev. B **69**, 064404 (2004).
 - ²⁰ O. I. Motrunich and T. Senthil, cond-mat/0407368.
 - ²¹ C. H. Chung, K. Voelker, and Y. B. Kim, Phys. Rev. B **68**, 094412 (2003).
 - ²² R. Coldea, D. A. Tennant, A. M. Tsvelik, and Z. Tylczynski, Phys. Rev. Lett. **86**, 1335 (2001).
 - ²³ R. Coldea, D. A. Tennant, and Z. Tylczynski, Phys. Rev. B **68**, 134424 (2003).
 - ²⁴ M. Greiner, O. Mandel, T. Esslinger, T. W. Hansch, and I. Bloch, Nature **415**, 39 (2002).
 - ²⁵ C. Honerkamp and W. Hofstetter, Phys. Rev. Lett. **92**, 170403 (2004).
 - ²⁶ S. Sachdev and R. Jalabert, Mod. Phys. Lett. B **4**, 1043 (1990).
 - ²⁷ S. Sachdev, Phys. Rev. B p. 12377 (1992).
 - ²⁸ N. Read and S. Sachdev, Phys. Rev. Lett. **62**, 1694 (1989).
 - ²⁹ P. Nikolic and T. Senthil, Phys. Rev. B **68**, 214415 (2003).
 - ³⁰ P. Nikolic and T. Senthil, cond-mat/0402262.
 - ³¹ P. Nikolic, cond-mat/0403332.
 - ³² F. D. M. Haldane, Phys. Rev. Lett. **61** (1988).
 - ³³ O. Tchernyshyov, R. Moessner, and S. L. Sondhi, cond-mat/0408498.